

Hiroshi Sakai
J. Umemura

Evaluation of molecular structure in Langmuir monolayers of zinc stearate and zinc 12-hydroxystearate by IR external reflection spectroscopy

Received: 21 March 2001
Accepted: 6 July 2001

H. Sakai (✉)
Heian Jogakuin (Saint Agnes') College
Nanpeidai, Takatsuki
Osaka-Fu 569-1092, Japan
e-mail: sakai@tk.heian.ac.jp
Tel.: +81-726-964924
Fax: +81-726-964919

J. Umemura
Institute for Chemical Research
Kyoto University
Uji, Kyoto-Fu 611-0011, Japan

Abstract In situ polarized Fourier transform IR external reflection spectra of Langmuir monolayers of zinc stearate and zinc 12-hydroxystearate on a water surface were recorded for various surface areas, and their molecular structures were estimated. In the zinc stearate monolayer, the wavenumbers and the absorbances of the antisymmetric and symmetric methylene stretching bands did not change during monolayer compression, which means that orientational and conformational changes of the hydrocarbon chain did not occur. However, wavenumber changes of

the antisymmetric and symmetric carboxylate stretching bands were observed during surface compression. The change in the binding nature of the zinc cation to the carboxylate group was speculated. Moreover, it was elucidated that the structure of the hydrocarbon chain in the zinc 12-hydroxystearate monolayer was different from that in the zinc stearate monolayer.

Keywords Langmuir monolayer · Fourier transform IR · External reflection spectroscopy · Zinc stearate · Zinc 12-hydroxystearate

Introduction

Langmuir monolayers at the air–water interface are susceptible to metal ions in the subphase, and the effect is reflected in π -A isotherms [1–3]. Some kinds of metal ions lead to condensation of the fatty acid monolayers, and without surface pressure two-dimensional crystals form. The molecular configuration in Langmuir monolayers with metal ions has attracted considerable interest because of many potential applications, especially to Langmuir–Blodgett films [4, 5]. However, a comprehensive understanding of the role of metal ions is still lacking at the molecular level.

Various methods have been applied to clarify the microscopic structure of Langmuir monolayers. Among those, IR spectroscopy has the advantage of being easy to use, nondestructive against samples, and sensitive to changes in the molecular conformation. So far, there have been many investigations of Fourier transform

(FT) IR external reflection spectra (ERS) of Langmuir monolayers under various conditions [6–27]; however, limited work has been conducted as far as the influence of metal ions on Langmuir monolayers is concerned. In previous work [9, 25] we measured the ERS of the Langmuir monolayers of cadmium stearate, and evaluated the molecular conformation and orientation, which was compared with stearic acid monolayers. Gericke and Hünerfuss [19] investigated the effect of cadmium, lead, and calcium ions on stearic acid monolayers, and discussed the interaction between these ions and the carboxylate group.

In the present work, we measured polarized FT-IR/ERS of the Langmuir monolayer of zinc stearate on the water surface for various surface areas, and evaluated the molecular structures. The zinc stearate monolayer at the air–water interface at a large surface area with no practical surface pressure has been studied by total-reflection X-ray absorption fine structure spectroscopy,

and the change of the coordination structure of the zinc ions has been reported [28]. The purpose of the present work is to clarify the structural changes under phase transitions that are represented in the π -A isotherms.

In addition, we also studied the Langmuir monolayer of zinc 12-hydroxystearate to be compared with zinc stearate, and with 12-hydroxystearic acid that was investigated previously [26]. This is not only for further understanding of the molecular structure in the zinc stearate monolayer, but also because there have been few studies of the Langmuir monolayers of bipolar molecules with metal ions.

Experimental

Stearic acid and 12-hydroxystearic acid were the same as reported previously [9, 26]. All the other reagents were either highly pure (above 98%) or of spectroscopic grade. Distilled water was prepared by a modified Mitamura Riken model PLS-DFR automatic lab still consisting of a reverse-osmosis module, an ion-exchange column, and a double distiller.

The Langmuir monolayers of zinc stearate and zinc 12-hydroxystearate were prepared on an aqueous solution of 1×10^{-3} M ZnCl_2 by spreading $11.3 \mu\text{l}$ 8.12×10^{-4} M chloroform solution of stearic acid and $11.9 \mu\text{l}$ 8.12×10^{-4} M benzene solution of 12-hydroxystearic acid, respectively. A trough with an $80 \times 22\text{-mm}^2$ effective surface area attached to a Specac 19650 monolayer/grazing angle accessory was used. An S.T. Japan model STJ-100 wire-grid polarizer with 1300 line/mm Al wires on KRS-5 was settled just above the water surface to optimize the polarization. FT-IR/ERS of Langmuir monolayers were recorded using a Nicolet Magna 850 FT-IR spectrophotometer equipped with a deuterated triglyceride sulfate detector with a resolution of 8 cm^{-1} . The incident angle was 42° with an s-polarized beam. First, the background spectrum was collected with 1,500 scans at the aqueous solution surface, and then the solution of stearic acid or 12-hydroxystearic acid was spread out. After waiting for 10 min to allow the solvent to completely evaporate, the Langmuir monolayer was compressed to various surface areas, and FT-IR/ERS were recorded with 300 scans.

The π -A isotherms were measured with a Wilhelmy balance attached to a Kyowa Interface Science model HBM-AP Langmuir trough. The compression velocity of stearic acid and zinc stearate was $0.0136 \text{ nm}^2 \text{ molecule}^{-1} \text{ min}^{-1}$, and that of 12-hydroxystearic acid and zinc 12-hydroxystearate was $0.0288 \text{ nm}^2 \text{ molecule}^{-1} \text{ min}^{-1}$. All the experiments were performed at 25°C .

Results and discussion

The π -A isotherms of stearic acid and zinc stearate at 25°C are shown in Fig. 1. In the stearic acid monolayer, the liquid-condensed L_2 phase and the super-liquid LS phase (more correctly solid phase) were observed [9, 29], while there was only an LS phase in the zinc stearate monolayer. In previous work [9, 25] we studied the Langmuir monolayers of stearic acid and cadmium stearate, and evaluated the molecular orientation angles. In the stearic acid monolayer, the orientation angle of the hydrocarbon chain from the surface normal decreased from 20° to almost 0° in the L_2 phase during

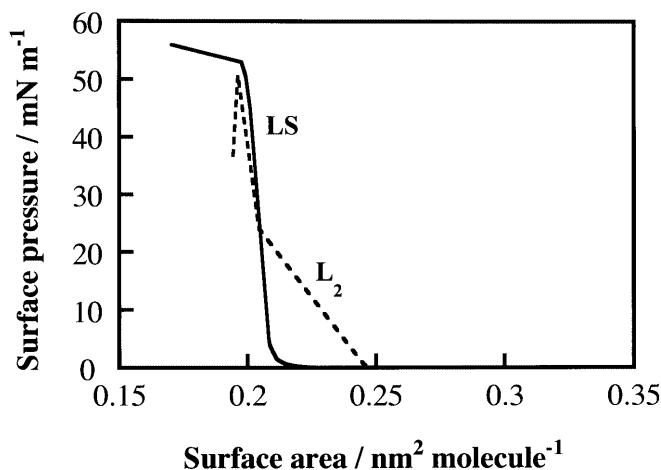


Fig. 1 π -A isotherms of zinc stearate (solid line) and stearic acid (broken line) on the water surface at 25°C

monolayer compression, and the chain was vertical in the LS phase. In the cadmium stearate monolayer, on the other hand, the orientation angle (near 0°) did not change during compression. The isotherm of zinc stearate was similar to that of cadmium stearate. It is expected that the hydrocarbon chain of zinc stearate stands almost perpendicular to the water surface, and does not change during compression.

The ERS of the Langmuir monolayers of zinc stearate between $4,000$ and 500 cm^{-1} for various surface areas are shown in Fig. 2. Antisymmetric and symmetric methylene stretching bands ($\nu_a \text{CH}_2$ and $\nu_s \text{CH}_2$) at about $2,914$ and $2,850 \text{ cm}^{-1}$, respectively, antisymmetric and symmetric carboxylate stretching bands ($\nu_a \text{COO}^-$ and $\nu_s \text{COO}^-$) at about $1,542$ and $1,398 \text{ cm}^{-1}$, respectively, a

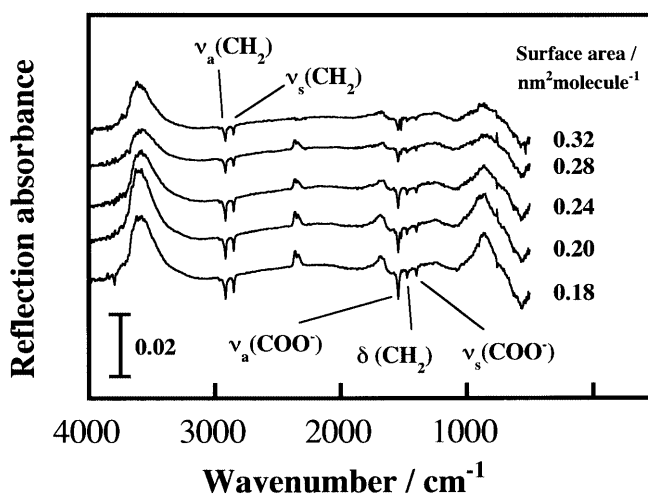


Fig. 2 Fourier transform IR external reflection spectra of a Langmuir monolayer of zinc stearate measured by an s-polarized beam for various surface areas

methylene scissoring band (δCH_2) at about $1,472\text{ cm}^{-1}$, and water bands at about $3,580$, $1,660$, and 850 cm^{-1} were observed. In the ERS measurements of Langmuir monolayers on the water surface, the reflection absorbance appears positive or negative (upward or downward) depending on the direction of the transition moment, the angle of incidence, and the polarization of the incident beam [7]. Under the present conditions (*s*-polarization), the observed IR bands of the monolayer show a negative reflection absorbance, while the water bands show a positive reflection absorbance. We have studied and discussed the water bands of Langmuir monolayer before [27].

It is known that the wavenumbers of the $\nu_a\text{CH}_2$ and $\nu_s\text{CH}_2$ bands are sensitive to the state of the molecular conformation and packing [9]. A plot of the wavenumbers of the $\nu_a\text{CH}_2$ and $\nu_s\text{CH}_2$ bands for the zinc stearate monolayer (Fig. 2) against the surface area is shown in Fig. 3. The wavenumbers of both bands did not change during compression. When the gauche conformer is rich, these frequencies appear at relatively high frequencies, e.g., $2,924$ and $2,854\text{ cm}^{-1}$, respectively. When the all-trans conformer is predominant, they appear at lower frequencies, e.g., $2,917$ and $2,850\text{ cm}^{-1}$ [9]. The observed antisymmetric CH_2 stretching frequency of $2,914\text{ cm}^{-1}$ is much lower than the value of $2,917\text{ cm}^{-1}$ previously observed for the octadecyl group of stearic acid or metal stearate [19]. The present value is rather close to the case of the coagel phase of the octadecyltrimethylammonium chloride/water system [30]. In the coagel phase of that system, the methylene chains take the trans-zigzag

conformation packed parallel with each other, and the hydrophilic part is in a fixed state. Therefore, a similar highly compact packing of the acyl chain is estimated in the present system. Since the zinc atom has a relatively small ionic or covalent radius among various divalent cations [31, 32], the condensation effect is strong [33].

The peak intensities of the $\nu_a\text{CH}_2$ and $\nu_s\text{CH}_2$ bands for the zinc stearate film shown in Fig. 2 are plotted against the surface area in Fig. 4. The intensity data were first calibrated for the surface density, since the peak intensity is related to the surface density, the molecular conformation, and the molecular orientation. The calibration was based on the difference in the surface density to a surface area of $0.2\text{ nm}^2\text{ molecule}^{-1}$. After the calibration, information about the molecular conformation and orientation can be extracted. The peak intensities of both bands did not change, although they somewhat scattered. This result indicates that neither the molecular conformation nor the molecular orientation of the hydrocarbon chain in the zinc stearate monolayer changed during compression.

The wavenumbers of $\nu_a\text{COO}^-$ and $\nu_s\text{COO}^-$ in the Langmuir monolayer of zinc stearate against the surface area are shown in Fig. 5. On monolayer compression, the wavenumber of the $\nu_a\text{COO}^-$ band increased from about $1,541\text{ cm}^{-1}$ to about $1,542.5\text{ cm}^{-1}$, while the wavenumber of the $\nu_s\text{COO}^-$ band decreased from about $1,399\text{ cm}^{-1}$ to about $1,397.5\text{ cm}^{-1}$. Although the spectral resolution itself is 8 cm^{-1} in this experiment, the accuracy of the peak position reading in the carboxylate stretching region is within 0.2 cm^{-1} ; therefore, the

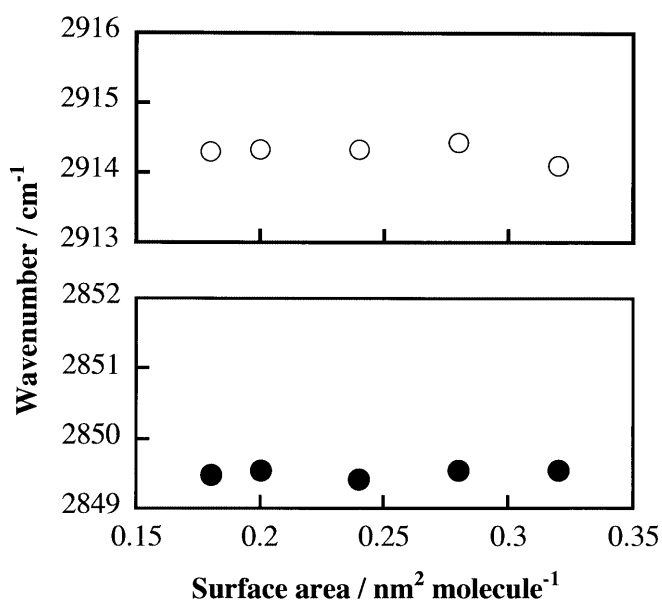


Fig. 3 Wavenumbers of $\nu_a\text{CH}_2$ (open circles) and $\nu_s\text{CH}_2$ (filled circles) in a Langmuir monolayer of zinc stearate versus surface area

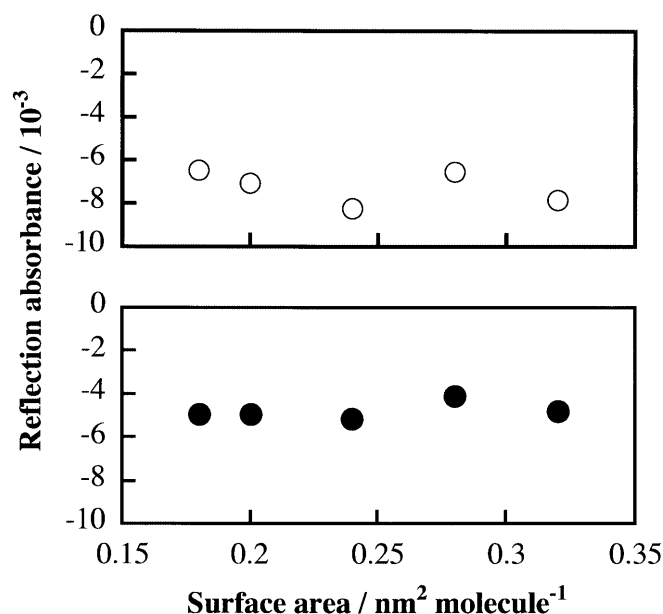


Fig. 4 Peak intensities of $\nu_a\text{CH}_2$ (open circles) and $\nu_s\text{CH}_2$ (filled circles) in a Langmuir monolayer of zinc stearate versus surface area

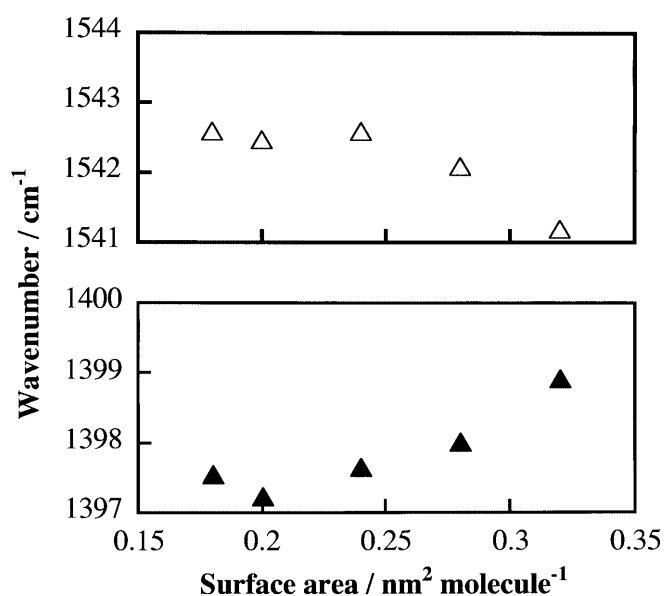


Fig. 5 Wavenumbers of $\nu_a\text{COO}^-$ (open triangles) and $\nu_s\text{COO}^-$ (filled triangles) in a Langmuir monolayer of zinc stearate versus surface area

wavenumber shifts indicate that some structural changes of the carboxylate group of zinc stearate occurred [34]. The $\nu_a\text{COO}^-$ wavenumber depends on the O–C–O angle, α , of the carboxylate group as follows [35]:

$$\nu_a\text{COO}^- = 1303 \sqrt{K \left(\frac{1}{m_O} + \frac{1 - \cos \alpha}{m_C} \right)}, \quad (1)$$

where K is the C–O stretching force constant in millidynes per angstrom, and m_O and m_C are the relative atomic masses of oxygen and carbon. Although this equation is oversimplified, the tendency is indicated. Substitutions of $K=7.2$ [36], $m_C=12.01$, $m_O=16.00$, and the previous $\nu_a\text{COO}^-$ wavenumbers into Eq. (1) increase α from 125.6° to 125.9° during the compression. In the case of the $\nu_s\text{COO}^-$ wavenumber, the sign of the $\cos \alpha$ term in Eq. (1) is positive [35]. As a result, on increasing the O–C–O angle, the wavenumber of the $\nu_s\text{COO}^-$ band decreases by a similar amount as the $\nu_a\text{COO}^-$ band.

Metal cations can bind to the carboxylate group in several ways. The first one is ionic binding. The second is the unidentate type, where a metal atom covalently binds to one of the carboxylate oxygen. The third is the chelate bidentate type, where a metal atom binds covalently to both oxygen atoms of the carboxylate group. The fourth is the bridging bidentate type, where two different metal atoms bind covalently to each of the oxygen atoms of the carboxylate group. Deacon and Phillips [37] have pointed out that the bonding type of metal acetates in the solid state can be classified by the difference (Δ) between the antisymmetric and symmetric

COO^- stretching frequencies, i.e., $\Delta(\text{unidentate}) > \Delta(\text{ionic}) = 164 \text{ cm}^{-1}$ [38] $> \Delta(\text{bridging bidentate}) > \Delta(\text{chelate bidentate})$. Tackett [39] has presented the correlation of these carboxylate frequencies with the cation radius and expanded them to the case of aqueous solutions. Nara et al. [40] have made ab initio molecular orbital calculations of some metal acetates and ascertained the order $\Delta(\text{unidentate}) > \Delta(\text{ionic}) > \Delta(\text{bidentate})$. It has also been demonstrated that such correlation is related to changes in the C=O bond lengths and the O–C–O angle [40]. Ishioka et al. [41] have shown that monoclinic anhydrous zinc acetate has $\Delta(\text{bridging bidentate})$ of 115 cm^{-1} only slightly larger than $\Delta(\text{chelate bidentate})$ of 113 cm^{-1} of zinc acetate dihydrate. They concluded that zinc stearate with $\Delta=141 \text{ cm}^{-1}$ has the bridging bidentate structure on the basis of the more-reliable key band of the COO^- rocking mode. It is reported that the carboxylate group is connected to the zinc ion by a covalent bond in the zinc stearate monolayer on the water surface [28]; therefore, the Δ value of the present work ($142\text{--}145 \text{ cm}^{-1}$) can be safely assigned to the bidentate structure. The Δ increase during surface compression may be assigned either to the chelating–bridging structural change or to the coordination number change [28] including hydration or dehydration processes. Anyway, the structural change occurs only around the carboxylate group on surface compression of the two-dimensional crystal of the zinc stearate Langmuir monolayer.

The π -A isotherms of 12-hydroxystearic acid and zinc 12-hydroxystearate at 25°C are shown in Fig. 6. Although 12-hydroxystearic acid has a wide plateau region, it disappears in the zinc 12-hydroxystearate. In previous work [26] we studied the Langmuir monolayer of 12-hydroxystearic acid and evaluated the molecular orientation. Upon monolayer compression from the plateau region to the solid-phase region, the

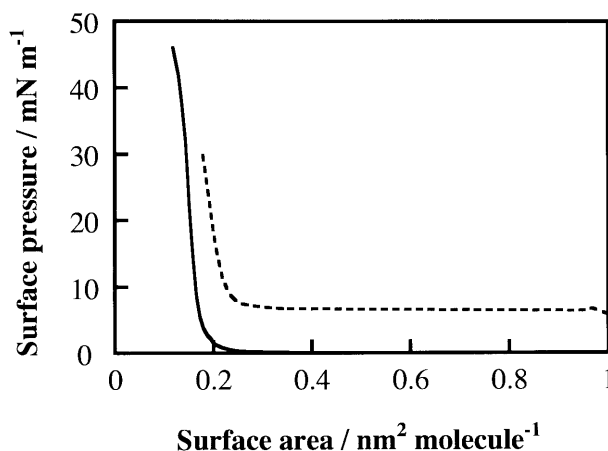


Fig. 6 π -A isotherms of zinc 12-hydroxystearate (solid line) and 12-hydroxystearic acid (broken line) on the water surface at 25°C

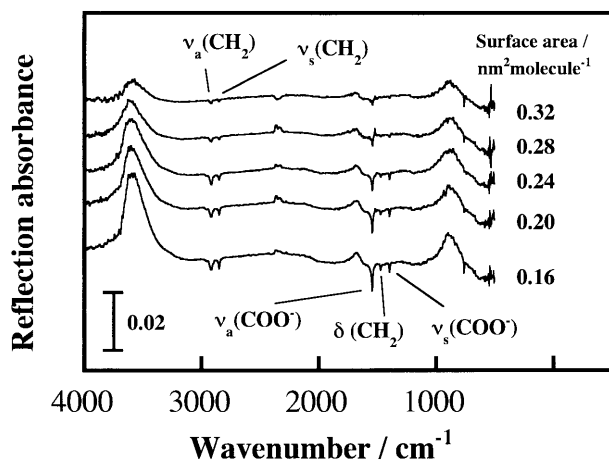


Fig. 7 Fourier transform IR external reflection spectra of a Langmuir monolayer of zinc 12-hydroxystearate measured by an s-polarized beam for various surface areas

orientation angle of the hydrocarbon chain from the surface normal decreased. The structure of the zinc 12-hydroxystearate monolayer would be much different from that of 12-hydroxystearic acid. The isotherm of zinc 12-hydroxystearate is rather similar to that of zinc stearate.

The ERS of the Langmuir monolayers of zinc 12-hydroxystearate between 4,000 and 500 cm^{-1} for various surface areas are shown in Fig. 7. At a first glance, it is observed that the peak intensities of both of the $\nu_a\text{CH}_2$ and $\nu_s\text{CH}_2$ bands are smaller than those of zinc stearate represented in Fig. 2. This means that the tilt angle of the hydrocarbon chain from the surface normal in the zinc 12-hydroxystearate monolayer is larger than that in the zinc stearate monolayer [25].

The wavenumbers of the $\nu_a\text{CH}_2$ and $\nu_s\text{CH}_2$ bands of zinc 12-hydroxystearate are plotted against the surface area in Fig. 8. Both bands decreased on monolayer compression. The frequencies of the antisymmetric CH_2 stretching band is also less than $2,917 \text{ cm}^{-1}$. The change seems to be due to the packing state change: the packing gets denser owing to the reorientational change of the hydroxy group into a more stable position during monolayer compression. This is contrasted with the case of zinc stearate where there is no steric hindrance by the hydroxy group. In addition, the structure of the carboxylate group also changed on monolayer compression in a similar manner to zinc stearate, which was inferred from the wavenumber change ($\nu_a\text{COO}^-$: from

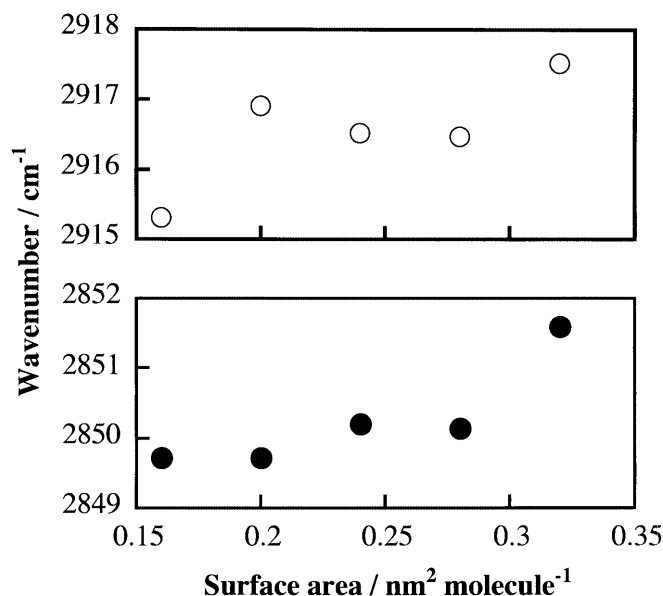


Fig. 8 Wavenumbers of $\nu_a\text{CH}_2$ (open circles) and $\nu_s\text{CH}_2$ (filled circles) in a Langmuir monolayer of zinc 12-hydroxystearate versus surface area

about $1,540 \text{ cm}^{-1}$ to about $1,542 \text{ cm}^{-1}$, $\nu_s\text{COO}^-$: from about $1,395 \text{ cm}^{-1}$ to about $1,394 \text{ cm}^{-1}$, not shown). In conclusion, both of the methylene and the carboxylate group structures changed in the Langmuir monolayer of zinc 12-hydroxystearate on compression.

Conclusion

In situ polarized FT-IR ERS of Langmuir monolayers of zinc stearate and zinc 12-hydroxystearate on the water surface were recorded for various surface areas and their molecular structures were estimated. In the zinc stearate monolayer, the orientation and conformation of the hydrocarbon chain did not change; however, the structure around the carboxylate group changed when the monolayer was compressed. Moreover, it was elucidated that the structure of the hydrocarbon chain in the zinc 12-hydroxystearate monolayer were different from those in the zinc stearate monolayer.

Acknowledgements This research was partially supported by a Grant-in-Aid for Scientific Research (B), 11440204, 1999–2001, and a Grant-in-Aid for Encouragement of Young Scientists, 11780088, 1999–2000, from the Japan Society for the Promotion of Science.

References

1. Gaines GL Jr (1966) Insoluble monolayers at liquid-gas interfaces. Interscience, New York
2. Yazdanian M, Yu H, Zografi G (1990) *Langmuir* 6:1093
3. Binks BP (1991) *Adv Colloid Interface Sci* 34:343
4. Robert GG (ed) (1990) *Langmuir-Blodgett films*. Plenum, New York
5. Ulman A (1991) An introduction to ultrathin organic films. Academic, Boston
6. Dluhy RA, Cornell DG (1985) *J Phys Chem* 89:3195
7. Dluhy RA (1986) *J Phys Chem* 90:1373
8. Mitchell ML, Dluhy RA (1988) *J Am Chem Soc* 110:712
9. Sakai H, Umemura J (1993) *Chem Lett* 2167
10. Gericke A, Michailov AV, Hünerfuss H (1993) *Vib Spectrosc* 4:335
11. Gericke A, Hünerfuss H (1993) *J Phys Chem* 97:12899
12. Buontempo JT, Rice SA (1993) *J Chem Phys* 98:5825
13. Buontempo JT, Rice SA (1993) *J Chem Phys* 98:5835
14. Blaudez D, Buffeteau T, Cornut JC, Desbat B, Escafre N, Pezolet M, Turlet JM (1993) *Appl Spectrosc* 47:869
15. Blaudez D, Buffeteau T, Cornut JC, Desbat B, Escafre N, Pezolet M, Turlet JM (1994) *Thin Solid Films* 242:146
16. Flach CR, Brauner JW, Mendelsohn R (1994) *Biophys J* 65:1994
17. Pastrana-Rios B, Flach CR, Brauner JW, Mautone AJ, Mendelsohn R (1994) *Biochemistry* 33:5121
18. Ren Y, Meuse CW, Hsu SL, Stidham HD (1994) *J Phys Chem* 98:8424
19. Gericke A, Hünerfuss H (1994) *Thin Solid Films* 245:74
20. Pastrana-Rios B, Taneva S, Keough KMW, Mautone AJ, Mendelsohn R (1995) *Biophys J* 69:2531
21. Flach CR, Prendergast FG, Mendelsohn R (1996) *Biophys J* 70:539
22. Sakai H, Umemura J (1996) *Chem Lett* 465
23. Flach CR, Gericke A, Mendelsohn R (1997) *J Phys Chem B* 101:58
24. Sakai H, Umemura J (1997) *Langmuir* 13:502
25. Sakai H, Umemura J (1997) *Bull Chem Soc Jpn* 70:1027
26. Sakai H, Umemura J (1998) *Langmuir* 14:6249
27. Umemura J, Sakai H (1999) In: Itoh K, Tasumi M (eds) *Fourier transform spectroscopy 12th International Conference*. Waseda University Press, Tokyo, pp 127-128
28. Watanabe I, Tanida H, Kawauchi S (1997) *J Am Chem Soc* 119:12018
29. Bibo AM, Peterson IR (1990) *Adv Mater* 2:309
30. Kawai T, Umemura J, Takenaka T, Kodama M, Seki S (1985) *J Colloid Interface Sci* 103:56
31. Rajagopal A, Kulkarni SK, Dhanabalan A, Major SS (1998) *Appl Surf Sci* 125:178
32. Pauling L (1960) *The nature of the chemical bond*, 3rd edn. Cornell University Press, New York
33. Tano T, Umemura J (1997) *Langmuir* 13:5718
34. Kamata T, Umemura J, Takenaka T, Koizumi N (1991) *J Phys Chem* 95:4092
35. Colthup NB, Daly LH, Wiberley SE (1990) *Introduction to infrared and Raman spectroscopy*, 3rd edn. Academic, New York, p 192
36. Grigor'ev AI (1963) *J Inorg Chem* 8:409
37. Deacon GB, Phillips RJ (1980) *Coord Chem Rev* 33:227
38. Nakamoto K (1997) *Infrared and Raman spectra of inorganic and coordination compounds*, 5th edn. Wiley, New York
39. Tackett JE (1989) *Appl Spectrosc* 43:483
40. Nara M, Torii H, Tasumi M (1985) *J Phys Chem* 100:19812
41. Ishioka T, Shibata Y, Takahashi M, Kanesaka I (1998) *Spectrochim Acta Part A* 54:1811